Macromolecular Nanotechnology

Atomistic Investigation of the Interfacial Mechanical Characteristics of Carbon Nanotube Reinforced Epoxy Composite

Q.L. Xiong, S.A. Meguid

PII: S0014-3057(15)00270-0
DOI: http://dx.doi.org/10.1016/j.eurpolymj.2015.05.006
Reference: EPJ 6907

To appear in: *European Polymer Journal*

Received Date: 30 January 2015
Revised Date: 29 April 2015
Accepted Date: 8 May 2015

Please cite this article as: Xiong, Q.L., Meguid, S.A., Atomistic Investigation of the Interfacial Mechanical Characteristics of Carbon Nanotube Reinforced Epoxy Composite, *European Polymer Journal* (2015), doi: http://dx.doi.org/10.1016/j.eurpolymj.2015.05.006

Atomistic Investigation of the Interfacial Mechanical Characteristics of Carbon Nanotube Reinforced Epoxy Composite

Q. L. Xiong and S. A. Meguid*

Mechanics and Aerospace Design Laboratory, Department of Mechanical and Industrial Engineering, University of Toronto, Toronto, Ontario M5S 3G8, Canada

Abstract

In this work, we investigate the interfacial mechanical characteristics of carbon nanotube (CNT) reinforced epoxy composite using molecular dynamics (MD) simulations. The MD simulations were carried out by developing two pull-out models; namely, the displacement-load model and the velocity-load model. The second-generation force field – polymer consistent force field (PCFF) – is used in the current MD simulations. The effects of various parameters, such as epoxy density, length and diameter of a CNT, the CNT-epoxy interfacial thickness, LJ cut-off distance and capping conditions of a CNT on the interfacial mechanical characteristics have also been investigated and discussed. The results from the present pull-out model, which are validated with earlier studies, reveal that (i) the interfacial shear strength (ISS) of the CNT-reinforced epoxy composite is improved with the increase in the epoxy density, (ii) the ISS of the CNT-reinforced epoxy composite decreases with the increase in the values of length and diameter of a CNT, and the thickness of CNT-epoxy matrix interface, (iii) the LJ cut-off distance has marginal effect on the ISS and the pull-out force of CNT, and (iv) incorporation of an end cap in the simulations results high initial pull-out peaks, which well correlate with the experimental findings.

Key words: Carbon nanotube; Epoxy nanocomposite; Interfacial mechanical characteristics; Molecular dynamics

*Corresponding author. Tel.: +1 (416) 978 5741; Fax: +1 (416) 978 7753.
E-mail address: meguid@mie.utoronto.ca (S.A. Meguid).

1. Introduction

In view of their superior mechanical, thermal and electrical properties [1-5], CNTs have emerged as the ideal reinforcements for multifarious applications in advanced nanocomposites [6-8]. It is a well-known fact that the load transfer between a CNT and the matrix plays an important role in the mechanical properties of the resulting nanocomposite. It is a complex process that depends largely on the interfacial bonding between the CNT reinforcement and the surrounding matrix. Fiber pull-out tests have been recognized as the standard method for evaluating the interfacial characteristics of composite materials. For example, the pull-out experiments of individual CNTs from the polymer matrix have been carried out by Cooper et al. [9] to evaluate the ISS of the resulting composite system. Kovalchuk et al. [10] studied the effect of functionalization of CNTs on the structural and mechanical properties of CNT reinforced polypropylene composites. They reported that better dispersion of CNTs within the polymer matrix can be achieved with covalent interactions between them. Their results also show that functionalization of CNTs leads to markedly improved plasticity and tensile modulus of the CNT polypropylene composite. Frankland et al. [11] investigated the influence of chemical cross-links on the shear strength of CNT reinforced polymer interfaces by using MD simulations. They concluded that the chemical functionalization of a CNT surface improves its interfacial adhesion with the surrounding polymer. Lachman and Wagner [12] studied the effect of the molecular nature of the nanoreinforced epoxy interface on the mechanical properties of the resulting composite and found that its toughness increases with the interfacial adhesion. Zheng et al. [13, 14] investigated the influences of sidewall modification and chemical functionalization of CNTs on the interfacial bonding characteristics of CNT-reinforced polymer composites using the molecular mechanics. Their results indicate that the appropriate functionalization of CNTs at low densities of functionalized carbon atoms drastically increase the interfacial bonding and shear stress between CNTs and the polymer matrix. Meguid and coworkers [15-17] investigated the effective elastic and interfacial properties of CNT-reinforced composites by using atomistic-based continuum (ABC) model. Their results show that the length, volume fraction, orientation and aspect ratio of the representative CNTs have significant effects on the elastic and interfacial properties of CNT-reinforced composites. They also reported that the ISS depends on the van der Waals (vdW) interaction density and decays significantly with the increase in the embedded CNT length in the polymer matrix. Li et al. [18] carried out a series of pull-out simulations of CNT to investigate

the interfacial properties between CNT and polymer matrix for two-phase CNT-polymer nanocomposites with only consideration of vdW interaction. A shear-lag model has been proposed by Ang and Ahmed [19] for assessing the interfacial characteristics of CNT-reinforced polymer matrix composites. Instead of considering any possible chemical bonding at the CNT-matrix interface, their study focuses on stress transferring mechanism of CNT arising from the combined effects of mechanical interlocking, Poisson's contraction, thermal mismatch and vdW interactions. Spanos et al. [20] developed a micromechanical hybrid finite element approach to study the stress transfer in CNT-reinforced composites. In their study, the interfacial effects between the two materials were simulated by appropriate stiffness variations defining a heterogeneous region. Chen et al. [21] presented an *in situ* electron microscopy nanomechanical study of the non-covalent vdW interfaces between individual CNTs and epoxy resins in conjunction with atomistic simulations.

Evidently, a number of analytical and experimental studies have been carried out by researchers to study the complexities of interfacial characteristics of CNT reinforced polymer composites. However, the correlations between these results are often difficult to evaluate and assess due to (i) the significant variation in the properties of the constituent phases, processing techniques and procedures, (ii) major differences in the adopted simulation techniques, and (iii) the way the pull-out problem is formulated and modeled in the numerical investigations. Some conclusions that are drawn from experimental studies have not been observed in numerical and analytical simulations. Specifically, experimental results exhibit high pull-out forces at the initial stage of a pull-out process. This is immediately followed by a sudden decay in the force until a CNT has fully been withdrawn from the polymer. On the contrary, the pull-out forces predicted by numerical simulations seem to increase up to a relatively fixed value until the last stages of a pull-out process. Therefore, several fundamental differences between experimental and numerical studies are worthy of investigation. In particular, little attention has been placed on the study of bonded interfaces and the effect of CNT diameter on the ISS. It is expected that if the polymer matrix fully embodies the embedded CNT, the additional vdW interactions at the base will serve to increase the initial pull-out force. It is therefore necessary to re-examine the bonded and non-bonded vdW mechanisms of CNT-reinforced composite and the key governing parameters to identify potential processing techniques that can be implemented in order to improve its ISS. Experimental measurements of the interfacial properties of CNT-polymer

composites are severely hindered by the length-scale involved in using CNTs. Therefore, an effective way of quantifying such properties is through the use of computational modeling techniques. In particular, we intend to investigate the effects of epoxy density, length and diameter of CNTs, interfacial thickness, LJ cut-off distance and capping conditions of a CNT on the ISS of the CNT-reinforced epoxy composite. For this purpose, we use MD simulations accounting for the nonbonded vdW and electrostatic interactions between CNTs and the surrounding epoxy matrix by incorporating the second-generation PCFF.

2. Force Fields and MD Simulations

We have generated the single polymer molecular chain and CNT by using VMD [22] as shown in Figs. 1(a) and 1(b). Subsequently, the Packmol software [23] is utilized to create a targeted molecular model for MD simulations as shown in Figs. 1(c) and 1(d). Figure 1 (c) and 1 (d) show the respective front and lateral views of the computational model of the CNT-reinforced composite. Large-Scale Atomic Molecular Massively Parallel Simulator (LAMMPS) [24] was then used to perform all MD simulations, and post processing of the simulations was performed using VMD. The second-generation PCFF [25] developed by Accelrys is used in the present study to model the interactions of atoms in the CNTs, the polymer and the CNT-polymer interface. The analytic forms (E_{pot}) of the energy expressions used in the PCFF are given below:

$$E_{pot} = E_{bond} + E_{angle} + E_{dihedral} + E_{vdWaals} + E_{Coulomb} \tag{1}$$

In the following we outline the details of the above equations. The PCFF bond description shown in Fig. 2 (a) obeys the following potential:

$$E_{bond} = K_2\left(r - r_0\right)^2 + K_3\left(r - r_0\right)^3 + K_4\left(r - r_0\right)^4 \tag{2}$$

The PCFF angle description shown in Fig. 2 (b) uses the following potential:

$$E_{angle} = E_a + E_{bb} + E_{ba} \tag{3}$$

$$E_a = H_2\left(\theta - \theta_0\right)^2 + H_3\left(\theta - \theta_0\right)^3 + H_4\left(\theta - \theta_0\right)^4 \tag{4}$$

$$E_{bb} = M\left(r_{ij} - r_1\right)\left(r_{jk} - r_2\right) \tag{5}$$

$$E_{ba} = N_1\left(r_{ij} - r_1\right)\left(\theta - \theta_0\right) + N_2\left(r_{jk} - r_2\right)\left(\theta - \theta_0\right) \tag{6}$$

while the PCFF dihedral effect shown in Fig. 2 (c) is described by the following potential:

$$E_{dihedral} = E_d + E_{mbt} + E_{ebt} + E_{at} + E_{aat} + E_{bb13} \quad (7)$$

$$E_d = \sum_{n=1}^{3} K_n \left[1 - \cos\left(n\phi - \phi_n\right)\right] \quad (8)$$

$$E_{mbt} = \left(r_{jk} - r_2\right)\left[A_1 \cos\left(\phi\right) + A_2 \cos\left(2\phi\right) + A_3 \cos\left(3\phi\right)\right] \quad (9)$$

$$E_{ebt} = \left(r_{ij} - r_1\right)\left[B_1 \cos\left(\phi\right) + B_2 \cos\left(2\phi\right) + B_3 \cos\left(3\phi\right)\right] + \left(r_{kl} - r_3\right)\begin{bmatrix} C_1 \cos\left(\phi\right) + C_2 \cos\left(2\phi\right) \\ + C_3 \cos\left(3\phi\right) \end{bmatrix} \quad (10)$$

$$E_{at} = \left(\theta_{ijk} - \theta_1\right)\left[D_1 \cos\left(\phi\right) + D_2 \cos\left(2\phi\right) + D_3 \cos\left(3\phi\right)\right] + \left(\theta_{jkl} - \theta_2\right)\begin{bmatrix} E_1 \cos\left(\phi\right) + E_2 \cos\left(2\phi\right) \\ + E_3 \cos\left(3\phi\right) \end{bmatrix} \quad (11)$$

$$E_{aat} = M\left(\theta_{ijk} - \theta_1\right)\left(\theta_{jkl} - \theta_2\right)\cos\left(\phi\right) \quad (12)$$

$$E_{bb13} = N\left(r_{ij} - r_1\right)\left(r_{kl} - r_3\right) \quad (13)$$

The van der Waals interaction potential shown in Fig. 2 (d) uses the standard 6-9 LJ potential, as given by

$$E_{vdW} = \varepsilon\left[2\left(\frac{\sigma}{r}\right)^9 - 3\left(\frac{\sigma}{r}\right)^6\right], \quad r < r_{cntoff} \quad (14)$$

Finally, the Coulombic interaction uses the following potential:

$$E_{Coul} = \sum_{i>j} \frac{q_i q_j}{\varepsilon r_{ij}} \quad (15)$$

where q is the atomic charge, ε is the dielectric constant, and r_{ij} is the i-j atomic separation distance, b and b' are the lengths of two adjacent bonds, θ is the two-bond angle, ϕ is the dihedral torsion angle, and χ is the out-of-plane angle. b_0, k_i (i = 2, 3, 4), θ_0, H_i (i = 2, 3, 4), ϕ_i^0, V_i (i = 1, 2, 3), $F_{bb'}$, b_0', $F_{\theta\theta}$, θ_0', $F_{b\theta}$, $F_{b\phi}$, F_i (i = 1, 2, 3), $F_{\theta\phi}$, $K_{\phi\theta\theta}$, A_{ij}, B_{ij} are fitted parameters from quantum mechanics calculations [26]. The values of different hydrocarbon and potential parameters appeared in the above equations are given in Tables 1–3.

A diglycidyl ether of bisphenol A (DGEBA) epoxy resin with triethylene tetramine (TETA) curing agent was used to create the current molecular models of cured epoxy (see Figs. 1 (c) and 1 (d)). In MD simulations, periodic boundary condition is applied in the x–y plane and the free boundary condition is assigned to the z-direction. Time steps were selected as 5.0 fs for all MD simulations. During the simulations, an axial displacement is applied to the rigidly constrained CNT and the equilibration process is carried out over 25 ps by using a time step of 0.5 fs in the Hoover style thermostat (NVT) ensemble. The periodic boundary conditions were

removed along the axial direction of the CNT and the matrix was constrained during the pull-out simulation [18]. The system was then equilibrated for another 25 ps in the isothermal–isobaric (NPT) ensemble at 300 K and 1 atm to generate a compressed structure with the correct density and residual stresses. This equilibration step resulted in an equilibrated structure with an average density of 1.09 g/cm3. At the end, the structure is again equilibrated for 25 ps in the Nose-Hoover style thermostat (NVT) ensemble at 300 K to obtain an equilibrated structure with minimum energy. These steps were repeated again in the subsequent axial displacement increments of the CNT. Two types of pull-out tests were carried out; namely, the displacement pull-out test and the velocity pull-out test. Several researchers studied the interfacial characteristics of CNT-reinforced composite using these tests [13–18, 21, 27–32, 35]. In the former test, the polymer matrix is constrained in the pull-out direction (z-direction) and is unconstrained in x- and y-directions. In this case, the CNT is pulled out in a series of steps, while equilibrating the system in between the steps to minimize its energy level. In the later test, a CNT is pulled out at the uniform velocity of 1×10^{-5} Å/fs until it is pulled out completely from the epoxy matrix. The pull-out force and the average ISS were then determined based on the work done during the pull-out test.

2.1 Model Validation: Comparisons with Existing MD Results

It is important at this stage to validate the molecular dynamics simulations. The predictions of the present MD simulations are compared against the pull-out results predicted by Li et al. [33]. Figure 3 depicts this comparison and it is observed that the results predicted herein by using the PCFF agree well with those predicted by Li et al. [33] using Condensed-Phase Optimized Molecular Potentials for Atomistic Simulation Studies force fields, known as COMPASS. On the other hand, significant differences are observed when using CVFF. This is attributed to the differences that exist between the different generations of force fields and the associated accuracy of representation of the interatomic representation. Therefore, PCFF has been used in the MD simulations of nanocomposite systems by several researchers [34-42] and some of their results are found to be in good agreement with experimental findings.

In the existing pull-out studies, mainely two types models are emplyed to investigate the interfacial charactersitics of CNT-reinforced polymer composites: the displacement pull-out model [13, 14, 18, 21, 33] using the molecular mechanics approach and the velocity pull-out

model [15–17] using ABC model. In the present work, we adopt MD simulation technique that incorporates the effect of temperature to perform the displacement and velocity pull-out tests. Subesequentely, a comparision has been made between the results predicted by these two tests. The total work done (w) by the pull-out force F_{pull} is equal to the total vdW pairwise energychange (ΔE_{int}) of a nanocomposite system for the specific distance pull-out displacement (Δx), such that,

$$\Delta E_{\text{int}} = \int_0^{\Delta x} F_{pull}(x)dx \tag{15}$$

Figure 4 illustrates these comparisons and it may be observed that the two sets of results are in excellent agreement. Accordingly, all subsequent MD simulations were carried out using the velocity pull-out model incorporating the PCFF. Figure 5 shows the pull-out forces and the vdW interaction energy during the pull-out process. It can be observed that the slope of vdW energy results well matches with that of the maximum value of the corresponding pull-out force implying the validation of the adopted approach.

The present work was further extended to validate the results predicted by the velocity pull-out model against those of the pull-out study of Zheng et al. [13]. For the comparison purpose, the average ISS has been estimated in terms of the change of the total energy [43]; as follows:

$$\Delta E = \pi r_{cnt} \tau_i L_e^2 \tag{17}$$

where ΔE denotes the difference in total energy of the CNT-reinforced epoxy nanocomposite system during the CNT pull-out process, r_{cnt} denotes the CNT radius, L_e is the embedded CNT length, and τ_i denotes the ISS. Referring to Fig. 3 and using Eq. (16), the calculated ISS for the present two-component epoxy system is 40.68 MPa. In comparison, Zheng et al. [13] predicted the non-bonded ISS ~33 MPa for a CNT of 5.9 nm in length embedded in the polyethylene matrix via MD simulations. These results are comparable, and any discrepancies can be attributed to differences in the CNT diameter, CNT length and polymer systems under consideration.

3. Results and Discussion

In this Section, the effects of various parameters, such as epoxy desity, length and diameter of a an embedded CNT, thickness of CNT-epoxy interface, LJ cut-off distance and CNT capping on

the interfacial mechanical characteristics of the CNT-reinforced epoxy composite are investigated.

3.1 Effect of Density of Epoxy

The density of the surrounding epoxy matrix significantly influences the number of vdW interactions between a CNT and the surrounding epoxy matrix. For this purpose, three types of epoxies with densities 0.6 g/cm^3, 1.09 g/cm^3 and 1.5 g/cm^3 are considered. For MD simulations, a rectangular box of size 5.0 nm × 5.0 nm × 6.641 nm of epoxy matrix is considered in which a CNT is embedded at the center. Unless otherwise mentioned, the value of the interfacial thickness between a CNT (10, 10) and the epoxy matrix is taken as 0.34 nm [33, 43, 44]. Figure 6 reveals that the ISS of the CNT-reinforced epoxy composite increases with the increase in the value of epoxy density. This is attributed to the fact that the vdW pairwise energy of CNT-epoxy interface and the pull-out forces increase with the increase in the epoxy density as illustrated in Figs. 7 and 8, respectively. This ultimately leads to the increase in the ISS of the resulting composite.

3.2 Effect of CNT Length

CNT length is a crucial parameter that significantly affects the composite properties. Several studies reported that the efficiency of interfacial load transfer in CNT-polymer composites significantly depends on the CNT length (see [44] and references therein). Hence, the effect of CNT length on the ISS of the CNT-reinforced epoxy composite is of importance to the present study. Three discrete values of CNT lengths are considered: 4.4 nm, 6.6 nm and 8.8 nm. It may be observed from Fig. 9 that the pull-out forces are almost the same for all CNT lengths. This is due to the fact that the cumulative resultant vdW force is normal to the axis of a CNT and hence to the direction of the loading. In comparison, the atoms of a CNT near its end have a component of the cumulative force opposing the pull-out force. Therefore, the embedded CNT length has no effect on the maximum pull-out force of the nonbonded CNTs interface.

Therefore, the maximum pull-out forces do not depend upon the length of the CNT. The figure also shows some sharp peaks in the pull-out profiles. These peaks are due to the random distributions of the atoms in the surrounding epoxy matrix. If the nanocomposite system is relaxed for a long time to attain an equilibrated position of the atoms in the epoxy matrix, the

pull-out profiles would exhibit a smoother and more consistent plateau regime. Furthermore, the effects of CNT length on the vdW interaction energy and the ISS of a nanocomposite are investigated as depicted in Figs. 10 and 11, respectively. These figures reveal that the vdW interaction energy of a nanocomposite system varies linearly with the length of the CNT length, while the ISS of the same decays with the increase in the CNT length.

3.3 Effect of CNT Diameter

In this work, the interfacial properties of the CNT-reinforced epoxy composite have so far been restricted to armchair CNT (10, 10) embedded in the epoxy matrix. The variation of the CNT diameter for a particular value of an embedded CNT length has been considered in this study. For this reason, three types of armchair CNTs are considered: (4, 4), (6, 6) and (10, 10). Keeping the length of the CNT constant as being 6.641 nm, the required pull-out forces for CNTs, the corresponding vdW interaction energy, and the ISS of the considered nanocomposite have been investigated as shown in Figs. 12-14. It may be observed from Fig. 12 that the pull-out forces required for a CNT increase with the increase in the CNT diameter. Figure 13 depicts that the vdW interaction energy increases linearly with that of the displacement of a CNT. On the other hand, the ISS of a nanocomposite decreases with the increase in the CNT diameter. These results demonstrate the advantage of using small diameter of CNTs, due to their significantly higher ISS values when compared to larger diameter of CNTs. This finding is consistent with the existing results reported by Wernik et al. [17].

3.4 Effect of Interfacial Thickness

Clearly, the reinforcing effect of the CNTs relies on an adequate load transfer at the CNT–matrix interface [21]. In this study, the interface thickness is defined as the separation distance between the CNT and the surrounding polymer atoms in the current unbonded (vdW) arrangement. A recent study reports that the polymer chains close to the binding interface with CNTs have more compact packing, higher orientation, and better mechanical properties compared with the bulk polymer [45]. The structure of the epoxy matrix at the vicinity of the CNT surface depends largely on the CNT-epoxy interface thickness. Therefore, an attempt has also been made to investigate the effect of the interfacial thickness on the interfacial mechanical characteristics of the CNT-reinforced epoxy composite. Different values of interfacial thickness ranging from 0.17

nm to 0.38 nm have been considered in earlier studies [46-48]. In our work, we varied the interfacial thickness from 0.25 nm to 0.45 nm; keeping the CNT length constant (6.64 nm). Figures 15 and 16 depict the effect of the interfacial thickness on the pull-out forces and the vdW interaction energy of a nanocomposite, respectively. It may be observed from these figures that the pull-out forces and the vdW interaction energy increase with the decrease in the interfacial thickness. This is attributed to the fact that CNT-epoxy interfacial vdW interactions become stronger with the decrease in the interfacial thickness, which eventually increases the cumulative resultant vdW force of an interface.

3.4 Effect of Lennard-Jones Cut-Off Distance

In MD, the LJ interatomic potential has typically been used to simulate vdW interactions, which is often truncated to reduce the computational cost. In earlier studies, many researchers considered the LJ cut-off distance to be approximately 1.0 nm [13-17, 33]. In order to investigate the effect of LJ cut-off distance on the pull-out force, we varied its distance from 0.80 nm to 1.2 nm for the fixed length of a CNT. Figures 17 and 18 demonstrate the effect of variation of LJ cut-off distance on the pull-out forces and the vdW interaction energy, respectively. These figures reveal that the LJ cut-off distance has marginal effect on the pull-out forces and the vdW interaction energy.

3.5 Effect of CNT Capping

Our pull-out profiles did not exhibit the initial characteristic peaks which are evident in the experimental pull-out profiles. In this Section, we investigate the interfacial mechanical characteristics of the CNT-reinforced epoxy composite incorporating the vdW interactions, which occur at the base of the embedded CNT caps. For such an investigation, we considered armchair (6, 6) CNT of length 6.64 nm embedded in the two-component DGEBA-TETA epoxy polymer. The CNT-epoxy interfacial thickness was taken to be 0.34 nm. Four different types of capping conditions are considered as shown in Fig. 19. The effect of the different capping conditions on the pull-out profiles and the vdW interaction energy during the pull-out process are shown in Figs. 20 and 21. These results reveal that capping has a significant effect on the interfacial mechanical characteristics of the CNT-reinforced epoxy composite. The most notable difference is in the presence of initial peaks in the pull-out profiles for CNTs with polymeric

end-caps. These peaks arise from the vdW interactions between the CNT and the epoxy at the base of the CNT when considering polymeric end-caps. A capped CNT with tight polymeric end-cap has a peak pull-out force three times larger than that of the base without the polymeric end-cap where neither the CNT cap nor the polymeric end-cap was considered. In addition, a capped CNT without polymeric end-cap does not seem to deviate much from the baseline. As such, we can conclude that the CNT caps do not significantly affect the magnitude of the pull-out forces unless fully surrounded by the matrix such that the additional atoms are given the opportunity to participate in these interactions. Furthermore, it may be observed from Fig. 21 that the capped CNT has no influence on the vdW interaction energy while the polymeric end-cap affects such energy.

4. Conclusions

In the present study, the interfacial mechanical characteristics of the CNT-reinforced epoxy composite, such as the ISS, pull-out force of CNT and vdW interaction energy between a CNT and the surrounding epoxy matrix, have been investigated using MD simulations. The atomistic interactions of the two-phase polymer considered were modeled using the second-generation force field - polymer consistent force field (PCFF). The results reveal that the ISS of the CNT-reinforced epoxy composite increases linearly with the increase in the epoxy density and decreases for greater values of length and diameter of CNT. The maximum values of pull-out force increases with the increase in the epoxy density, the diameter of CNT and LJ cut-off distance, but decreases with the increase in the CNT-epoxy interfacial thickness. On the other hand, it is found that the length of CNT does not influence the maximum value of the pull-out force. An examination of polymeric and CNT capping conditions revealed that incorporation of an end cap in the simulation yields high initial pull-out peaks indicating that capping improves the interfacial mechanical properties of CNT-reinforced composites. These findings have a direct bearing on the design and fabrication of CNT-reinforced composites.

Acknowledgement:

The authors wish to thank the Natural Sciences and Engineering Research Council of Canada and Discovery Accelerated Supplement for their kind financial support of the current studies. The authors also express their thanks to Dr. Shailesh I. Kundalwal for helpful discussions.

References

[1] Teacy MMJ, Ebbesen TW, Gibson JM. Exceptionally high Young's modulus observed for individual carbon nanotubes. Nature 1996; 381(6584): 678-680.

[2] Yakobson BI, Brabec CJ, Bernholc J. Nanomechanics of carbon tubes: Instabilities beyond linear response. Phys Rev Lett 1996; 76(14):2511-2514.

[3] Che JW, Cagin T, Goddard WA. Thermal conductivity of carbon nanotubes. Nanotechnology 2000; 11(2): 65–69.

[4] Berber S, Kwon Y, Tomanek D. Unusually high thermal conductivity of carbon nanotubes. Phys Rev Lett 2000; 84(20): 4613-4616.

[5] Ebbesen TW, Lezec HJ, Hiura H, Bennet JW, Ghaemi HF, Thio T. Electrical conductivity of individual carbon nanotubes. Nature 1996; 382, 54-56.

[6] Latibari ST, Mehrali M, Mottahedin L, Fereidoon A, Metselaar HSC. Investigation of interfacial damping nanotube-based composite. Compos Part B 2013; 50, 354–361.

[7] Kundalwal SI and Ray MC. Effect of carbon nanotube waviness on the effective thermoelastic properties of a novel continuous fuzzy fiber reinforced composite. Compos Part B 2014; 57, 199–209.

[8] Kundalwal SI, Ray MC and Meguid SA. Shear lag model for regularly staggered short fuzzy fiber reinforced composite. ASME J App Mech 2014; 091001.

[9] Cooper CA, Cohen SR, Barber AH, Wagner HD. Detachment of carbon nanotubes from a polymer matrix. Appl Phys Lett 2002; 81, 3873.

[10] Kovalchuk AA, Shevchenko VG, Shchegolikhin AN, Nedorezova PM, Klyamkina AN, Aladyshev AM. Effect of carbon nanotube functionalization on the structural and mechanical properties of polypropylene/MWCNT composites. Macromolecules 2008; 41, 7536.

[11] Frankland SJV, Caglar A, Brenner DW, Griebel M. Molecular simulation of the influence of chemical cross-links on the shear strength of carbon nanotube-polymer interfaces. J Phys Chem B 2002; 106, 3046.

[12] Lachman N, Daniel WH. Correlation between interfacial molecular structure and mechanics in CNT/epoxy nano-composites. Compos Part A 2010; 41, 1093.

[13] Zheng Q, Xia D, Xue Q, Yan K, Gao X, Li Q. Computational analysis of effect of modification on the interfacial mechanical characteristics of a carbon nanotube-polyethylene composite system. Appl Surf Sci 2009; 255, 3534–3543.

[14] Zheng Q, Xue Q, Yan K, Gao X, Li Q, Hao L. Effect of chemisorption on the interfacial bonding characteristics of carbon nanotube–polymer composites. Polymer 2008; 49, 800.

[15] Meguid SA, Wernik JM, Cheng ZQ. Atomistic-based continuum representation of the effective properties of nano-reinforced epoxies. Int J Solids Struct 2010; 47, 1723–1736.

[16] Wernik JM, Meguid SA. Multiscale modeling of the nonlinear response of nano-reinforced polymers. Acta Mech 2011; 217, 1–16.

[17] Wernik JM, Cornwell-Mott BJ, Meguid SA. Determination of the interfacial properties of carbon nanotube reinforced polymer composites using atomistic-based continuum model. Int J Solids Struct 2012; 49, 1852–1863.

[18] Li Y, Liu Y, Peng X, Yan C, Liu S, Hu N. Pull-out Simulations on Interfacial Properties of Carbon Nanotube-reinforced Polymer Nanocomposites. Comput Mater Sci 2011; 50, 1854–1860.

[19] Ang KK, Ahmed KS. An improved shear-lag model for carbon nanotube reinforced polymer composites. Compos Part B 2013; 50, 7–14.

[20] Spanos KN, Georgantzinos SK, Anifantis NK. Investigation of stress transfer in carbon nanotube reinforced composites using a multi-scale finite element approach. Compos Part B 2014; 63, 85–93.

[21] Chen X, Zhang L, Zheng M, Park C, Wang X, Ke C. Quantitative nanomechanical characterization of the van der Waals interfaces between carbon nanotubes and epoxy. Carbon 2015; 82, 214–228.

[22] Humphrey W, Dalke A, Schulten K. VMD: Visual molecular dynamics, J Mol Graphics 1996; 14, 33.

[23] http://www.ime.unicamp.br/~martinez/packmol/

[24] Plimpton S. Fast Parallel Algorithms for Short-Range Molecular Dynamics. J Comput Phys 1995; 117, 1-19.

[25] Sun H, Mumby SJ, Maple JR, Hagler AT. An abi initio CFF90 all-atom force field for polycarbonates. J Amer Chem Soc 1994; 116, 2978–2987.

[26] http://accelrys.com/products/materials-studio/polymers-and-classical-simulation-software.html

[27] Gou J, Minaie B, Wang B, Liang Z, Zhang C. Computational and experimental study of interfacial bonding of single-walled nanotube reinforced composites. Comput Mater Sci 2004; 31; 225–236.

[28] Chowdhury SC, Okabe T. Computer simulation of carbon nanotube pull-out from polymer by the molecular dynamics method. Compos Part A 2007; 38, 747–754.

[29] Al-Ostaz A, Pal G, Mantena PR, Cheng A. Molecular dynamics simulation of SWCNT-polymer nanocomposite and its constituents. J Mater Sci 2008; 43, 164–173.

[30] Zheng Q, Xue Q, Yan K, Gao X, Li Q, Hao L. Influence of chirality on the interfacial bonding characteristics of carbon nanotube polymer composites. J Appl Phys 2008; 103, 044302.

[31] Zheng Q, Xia D, Xue Q, Yan K, Gao X, Li Q. Computational analysis of effect of modification on the interfacial characteristics of a carbon nanotube- polyethylene composites system. Appl Surf Sci 2009; 255, 3524–3543.

[32] Rahmat M, Hubert P. Pull-out simulations on interfacial properties of carbon nanotube-reinforced polymer nanocomposites. Compos Sci Technol 2011; 72, 72–84.

[33] Li Y, Hu N, Yamamoto G, Wang Z, Hashida T, Asanuma H, Dong C, Arai M, Fukunaga H. Molecular mechanics simulation on sliding behavior between nested walls in a multi-walled carbon nanotube. Carbon 2010; 48, 2934–2940.

[34] Lordi V and Yao N. Molecular mechanics of binding in carbon-nanotube– polymer composites. J Mater Res 2000; 15, 2770–2779.

[35] Fan HB, Yuen MMF. Material properties of the cross-linked epoxy resin compound predicted by molecular dynamics simulation. Polymer 2007; 48, 2174–2178.

[36] Lim SY, Sahimi M, Tsotsis TT, Kim N. Molecular dynamics simulation of diffusion of gases in a carbon-nanotube–polymer composite. Phys Rev 2007; 76, 011810.

[37] Hu M, Keblinski P, Schelling PK. Kapitza conductance of silicon–amorphous polyethylene interfaces by molecular dynamics simulations. Phys Rev 2009; 79, 104305.

[38] Yang S, Yu S, Kyoung W, Han D-S, Cho M. Multiscale modeling of size-dependent elastic properties of carbon nanotube/polymer nanocomposites with interfacial imperfections. Polymer 2012; 53, 623–633.

[39] Zaminpayma E, Mirabbaszadeh K. Investigation of molecular interaction between single-walled carbon nanotubes and conjugated polymers. Polym Compos 2012; 33, 548–554.

[40] Rahman R, Foster JT, and Haque A. Molecular Dynamics Simulation and Characterization of Graphene− Cellulose Nanocomposites. J Phys Chem A 2013; 117, 5344−5353.

[41] Rahman R. The role of graphene in enhancing the stiffness of polymeric material: A molecular modeling approach. J App Phys 2013; 113, 243503.

[42] Yang S, Yu S, Cho M. Influence of Thrower–Stone–Wales defects on the interfacial properties of carbon nanotube/polypropylene composites by a molecular dynamics approach. Carbon; 55, 133–143.

[43] Liao K, Li S. Characteristics of carbon nanotube-polystyrene interface. Appl Phys Lett 2001; 79, 4225–4227.

[44] Wang X, Jiang Q, Xu W, Cai W, Inoue Y, Zhu Y. Effect of carbon nanotube length on thermal, electrical and mechanical properties of CNT/bismaleimide. Carbon 2013; 53, 145–152.

[45] Liu Y, Kumar S. Polymer/carbon nanotube nano composite fibers – a review. ACS Appl Mater Interfaces 2014; 6, 6069–6087.

[46] Hu N, Fukunaga N, Lu C, Kameyama M, Yan M. Prediction of elastic properties of carbon nanotube reinforced composites. Proc R Soc A 2005; 461, 1685–1710.

[47] Li CY, Chou TS. Multiscale modeling of compressive behavior of carbon nanotube/polymer composites. Compos Sci Technol 2006; 66, 2409–2414.

[48] Montazeri A, Naghdabadi R. Investigation the stability of SWCNT-polymer composites in the presence of CNT geometrical defects using multiscale modeling. Proceedings of the Fourth International Conference on Multiscale Materials Modeling. 2008; 163–166.

List of Tables

Table 1 Non-bonded LJ parameters

	ε (kcal/mol)	**σ (Å)**
C-C	0.0540000000	4.0100000000
H-H	0.0200000000	2.9950000000
O-O	0.2400000000	3.5350000000
N-N	0.0650000000	4.0700000000

Table 2 Bond parameters

	r_0 (Å)	**K_2 (ev/Å^2)**	**K_3 (ev/Å^3)**	**K_4 (ev/Å^4)**
C-C	1.5300	299.6700	-501.7700	679.8100
C-H	1.1010	345.0000	-691.8900	844.6000
C-O	1.4200	400.3954	-835.1951	1313.0142
C-N	1.4570	365.8052	-699.6368	998.4842
N-H	1.0060	466.7400	-1073.6018	1251.1056

Table 3 Angle parameters

	θ_0(degrees)	**H_2 (ev/radian^2)**	**H_3 (ev/radian^3)**	**H_4 (ev/ radian^4)**
C-C-C	112.6700	39.5160	-7.4430	-9.5583
C-C-H	110.7700	41.4530	-10.6040	5.1290
C-C-O	111.2700	54.5381	-8.3642	-13.0838
C-O-C	104.5000	35.7454	-10.0067	-6.2729
H-C-H	107.6600	39.6410	-12.9210	-2.4318
H-C-O	108.7280	58.5446	-10.8088	-12.4006
O-C-C	111.2700	54.5381	-8.3642	-13.0838
H-C-N	110.6204	51.3137	-6.7198	-2.6003
C-C-N	111.9100	60.7147	-13.3366	-13.0785
C-N-C	112.4436	47.2337	-10.6612	-10.2062

List of Figures

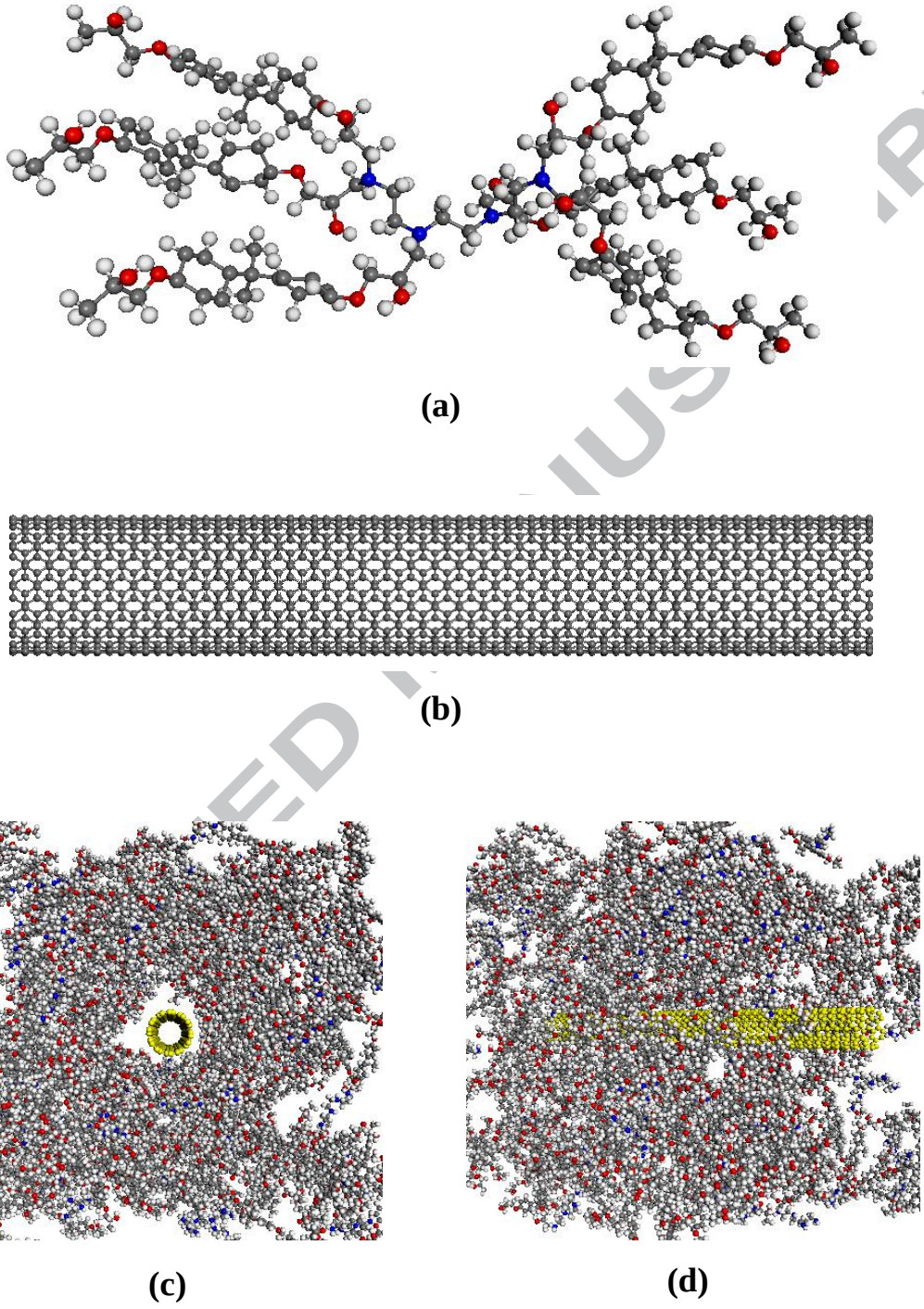

Fig. 1 – (a) Molecular model of a single DGEBA-TETA epoxy chain (The hydrogen, carbon, oxygen and nitrogen atoms of the epoxy chain are presented by white, grey, red and blue colors, respectively.); (b) molecular model of a single-walled CNT; (c) front and (d) lateral views of the computational model of the CNT- DGEBA-TETA composite.

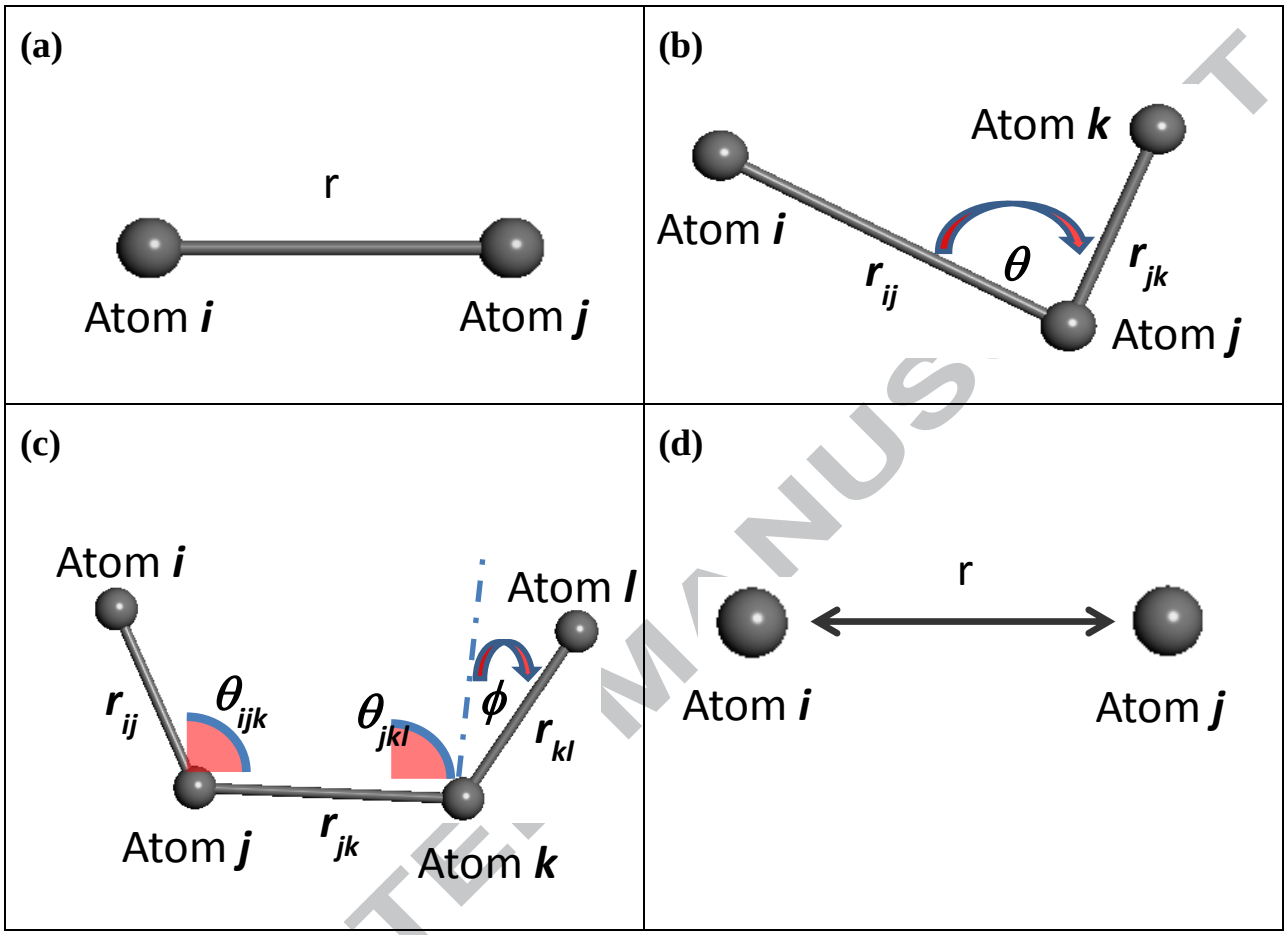

Fig. 2 - Schematics of the different PCFF terms (a) bond stretching, (b) two-bond angle, (c) a dihedral bond-torsion, and (d) a vdW interaction terms.

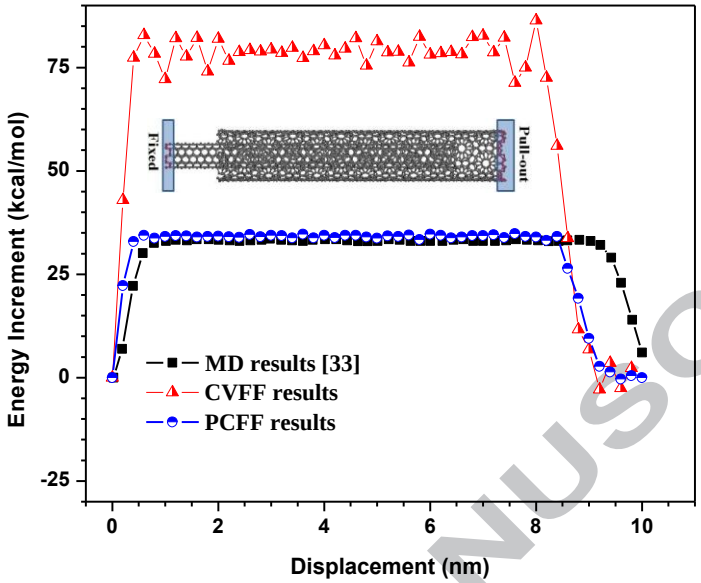

Fig. 3 - Comparisons of predicted results using different force fields.

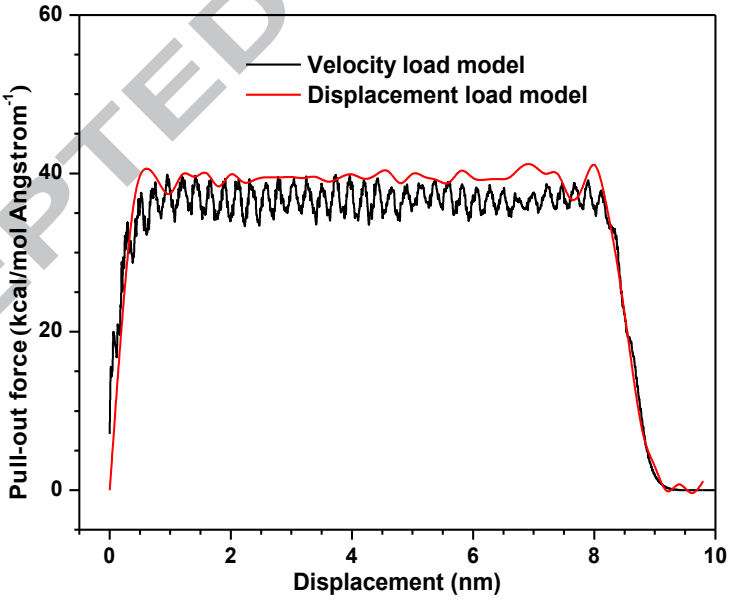

Fig. 4 - Comparison of the results for the pull-out forces required for a CNT predicted by the velocity and displacement pull-out models.

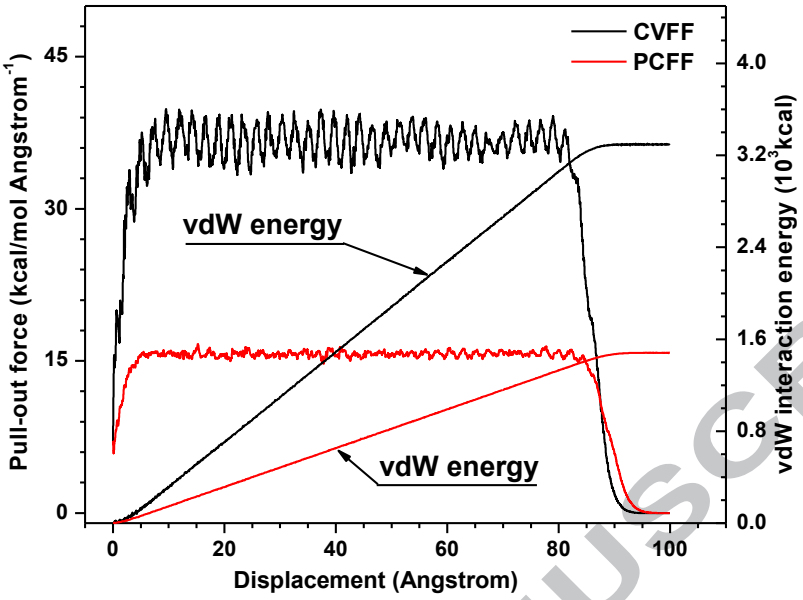

Fig. 5 - Variation of the pull-out forces and the vdW interaction energy during the pull-out process.

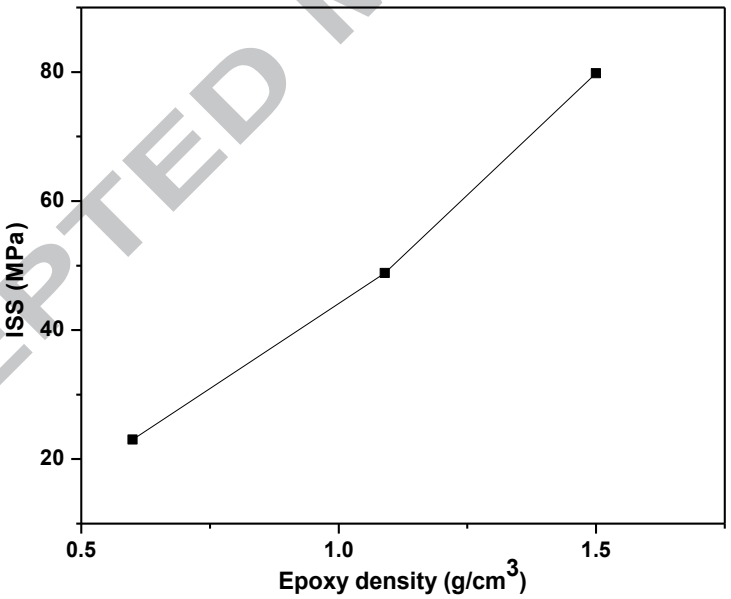

Fig. 6 - Effect of variation of epoxy density on the ISS of the CNT-reinforced epoxy composite.

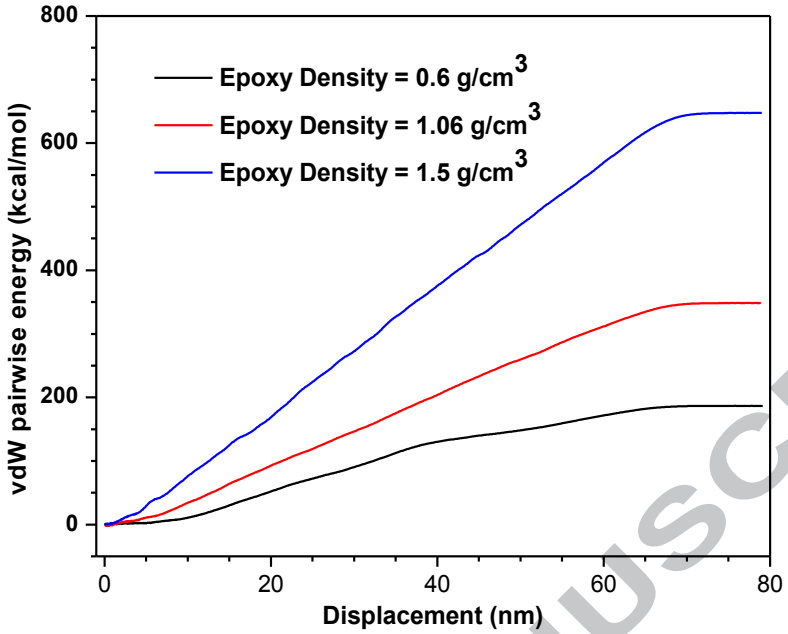

Fig. 7 - Effect of variation of epoxy density on the vdW interaction energy during the pull-out process.

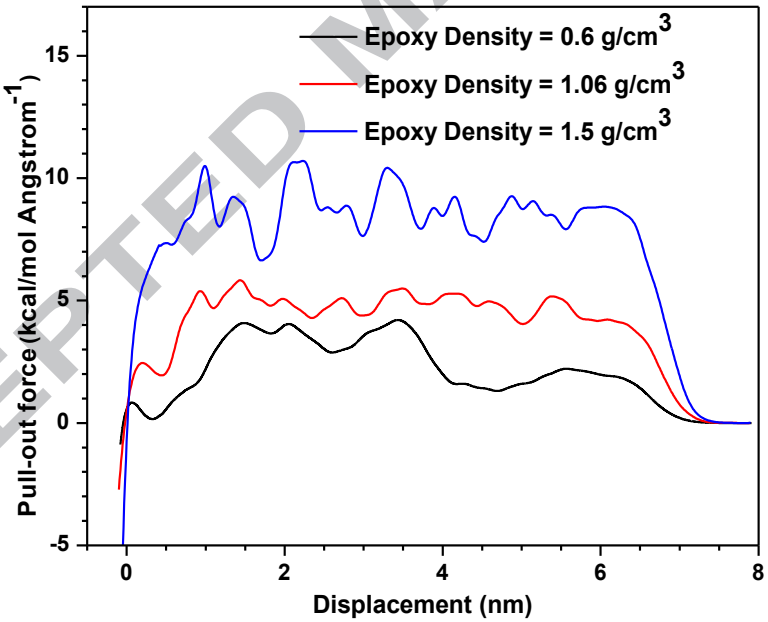

Fig. 8 - Effect of variation of epoxy density on the pull-out forces during the pull-out process.

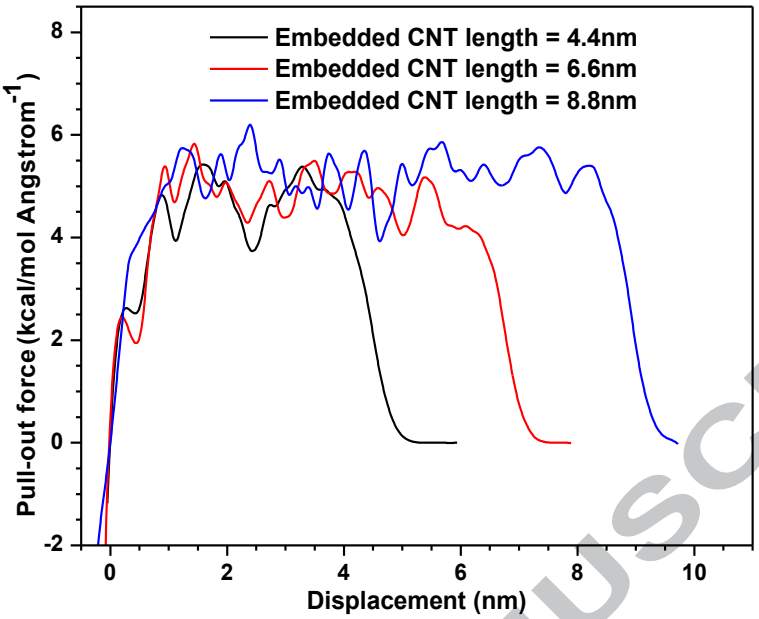

Fig. 9 - Effect of variation of CNT length on the pull-out forces during the pull-out process.

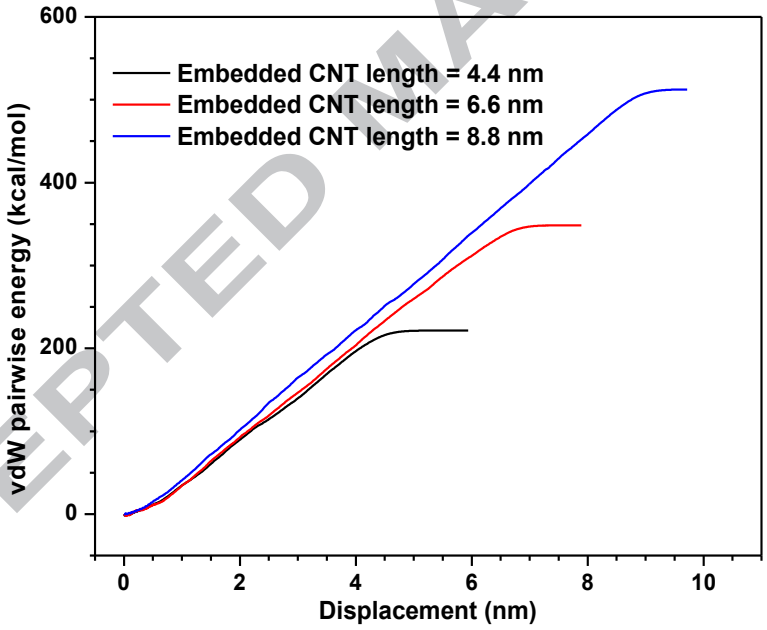

Fig. 10 - Effect of variation of CNT length on the vdW interaction energy during the pull-out process.

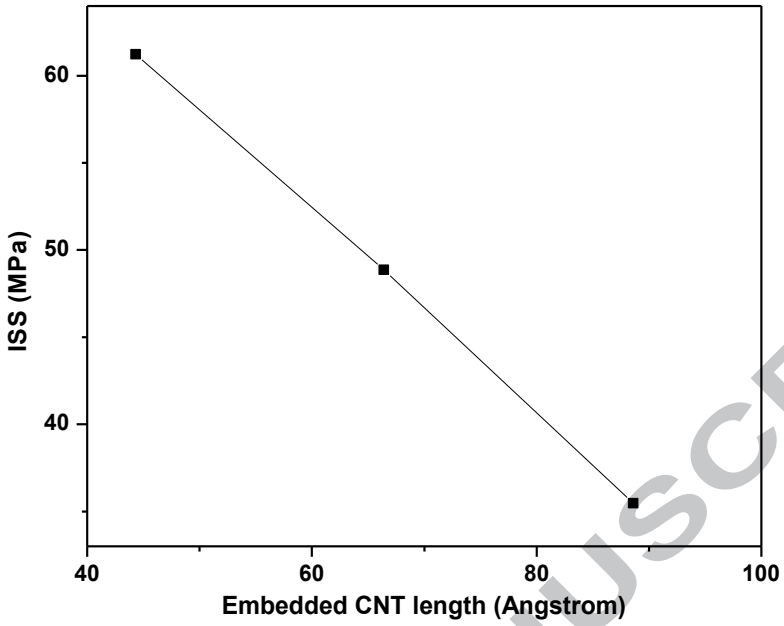

Fig. 11 - Effect of CNT length on the ISS of the CNT-reinforced epoxy composite.

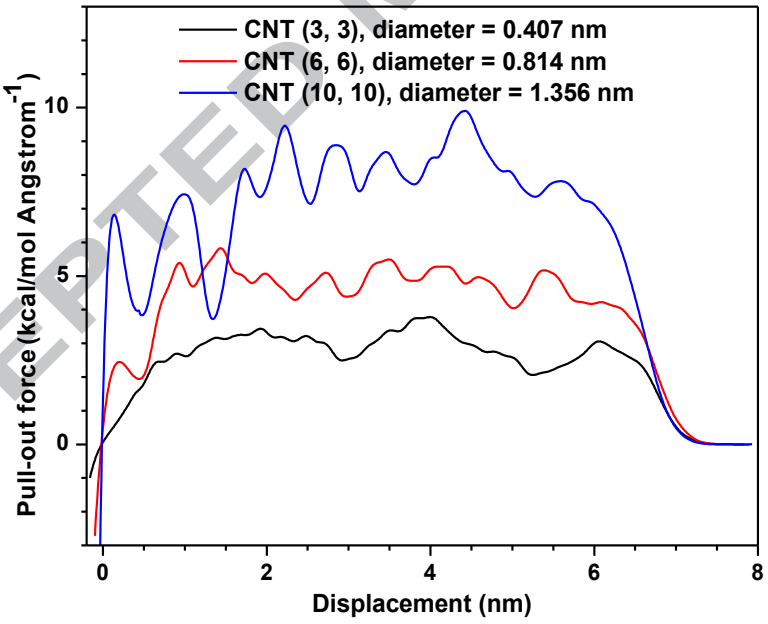

Fig. 12 - Effect of variation of CNT diameter on the pull-out forces during the pull-out process.

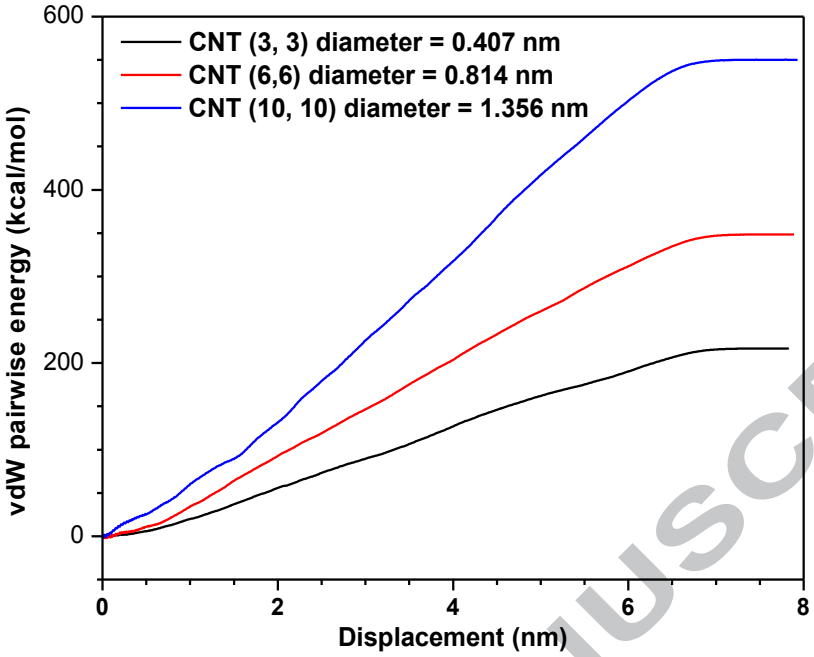

Fig. 13 - Effect of variation of CNT diameter on the vdW interaction energy during the pull-out process.

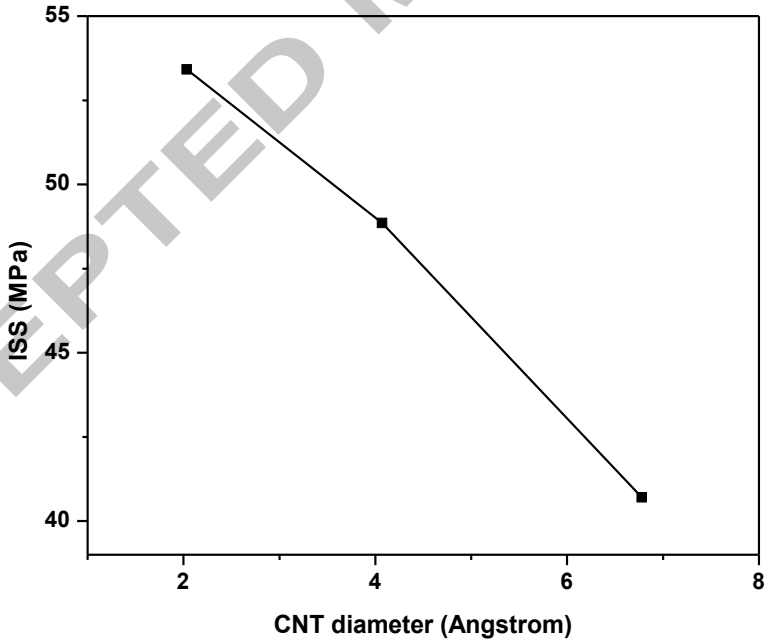

Fig. 14- Effect of variation of CNT diameter on the ISS of the CNT-reinforced epoxy composite.

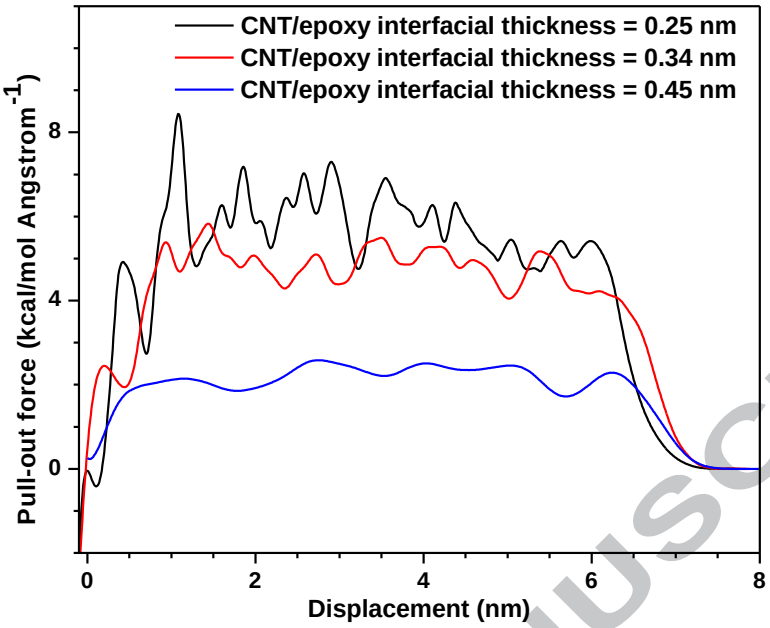

Fig. 15 - Effect of variation of CNT-epoxy interfacial thickness on the pull-out forces during the pull-out process.

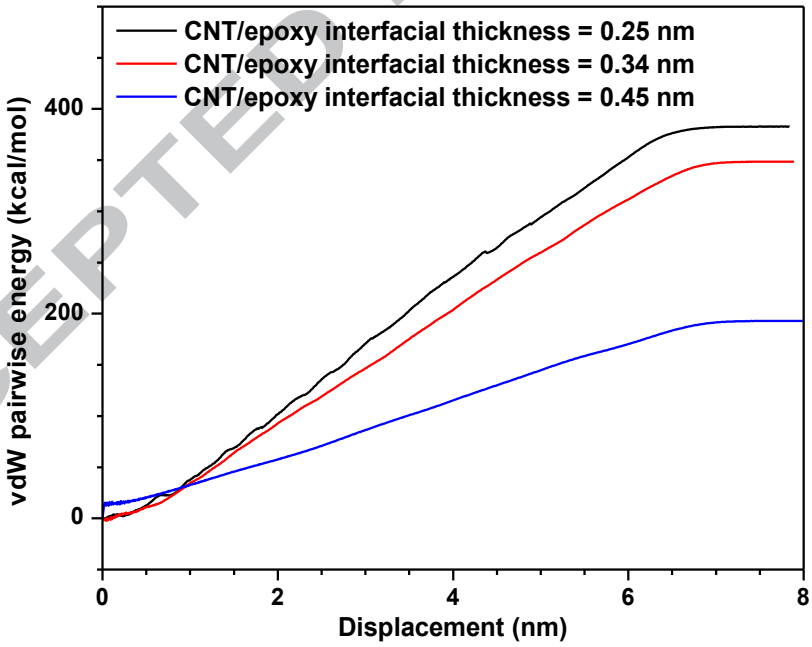

Fig. 16 - Effect of variation of CNT-epoxy interfacial thickness on the vdW interaction energy during the pull-out process.

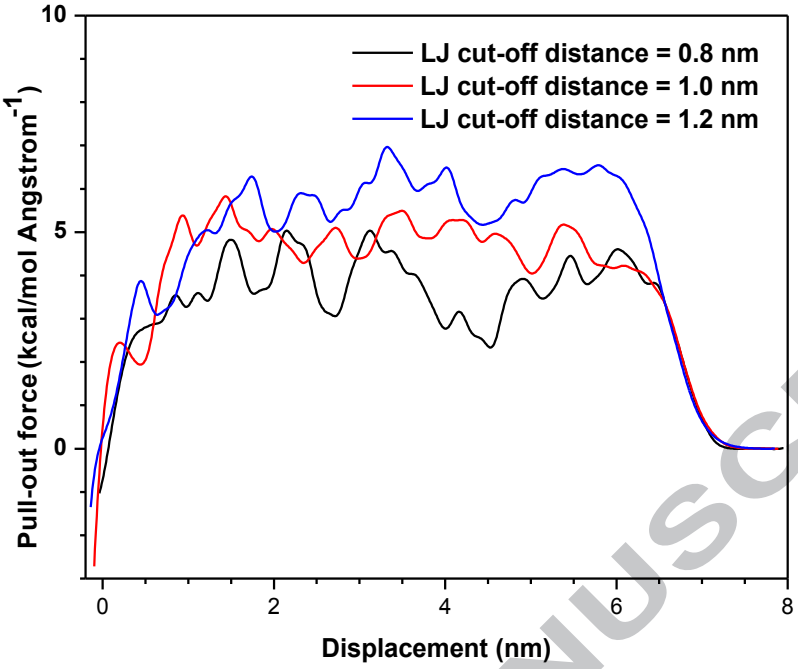

Fig. 17 - Effect of variation of LJ cut-off distance on the pull-out forces during the pull-out process.

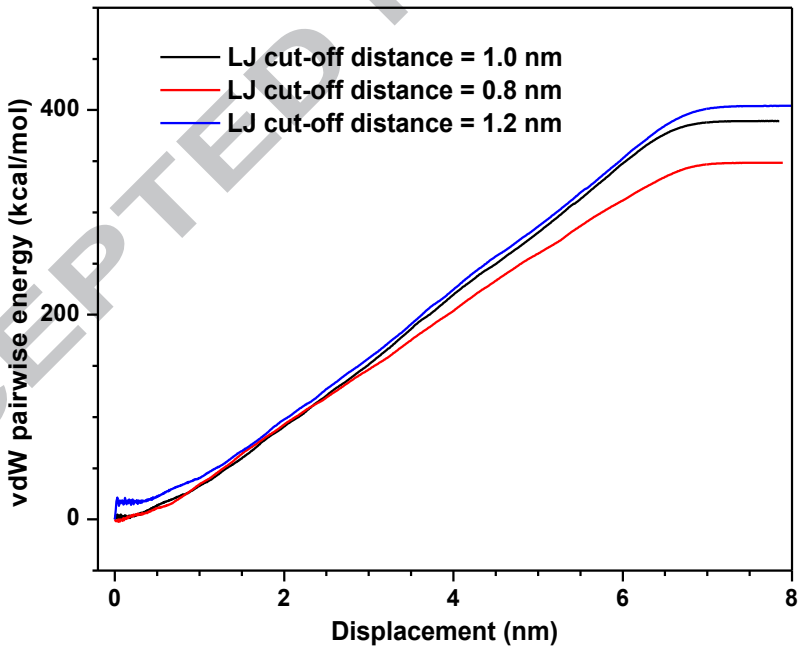

Fig. 18- Effect of variation of LJ cut-off distance on the vdW interaction energy during the pull-out process.

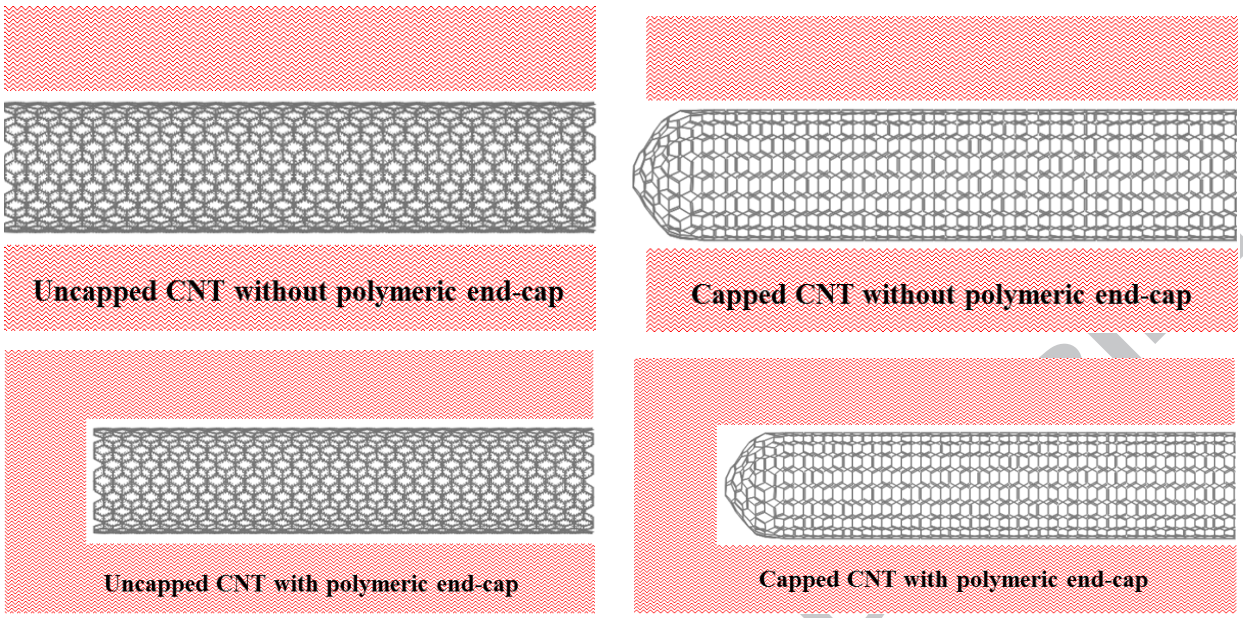

Fig. 19 - Different capping conditions of CNT- epoxy nanocomposites.

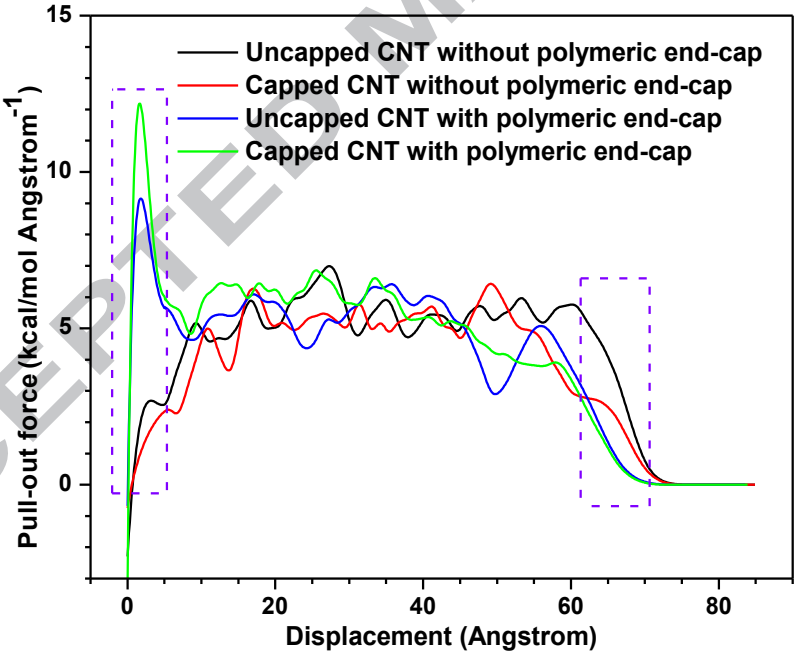

Fig. 20- Effect of different capping conditions on the pull-out forces during the pull-out process.

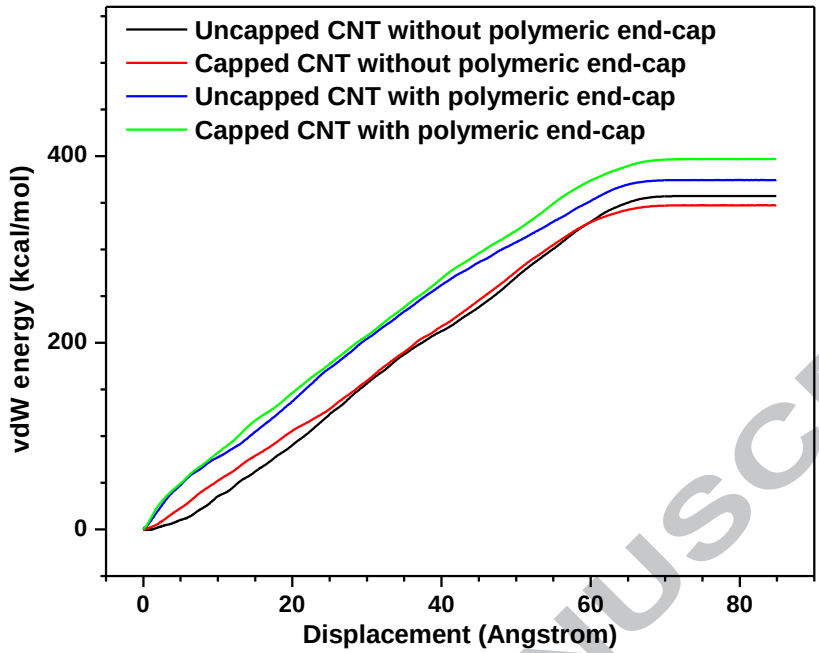

Fig. 21 - Effect of different capping conditions on vdW interaction energy during the pull-out process.

Graphical abstract

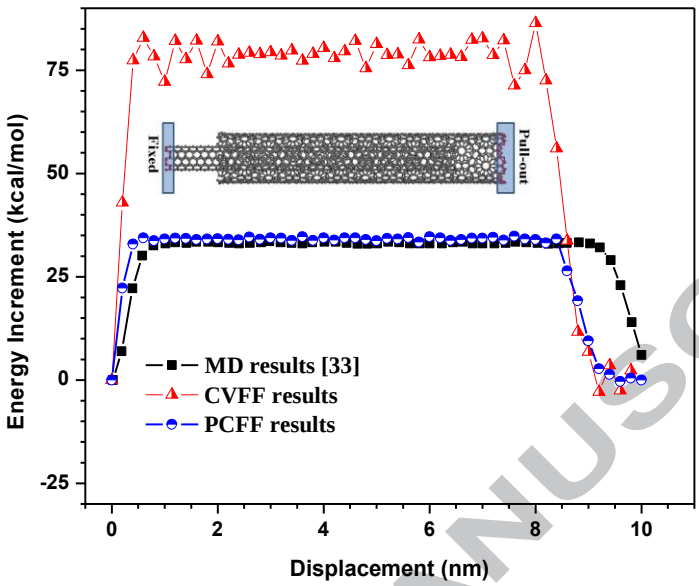

Highlights

- Load transfer in nanocomposites is governed by the interface strength
- Investigated the interface strength of CNT-epoxy composites using pull-out tests and MD
- The work reveals that the ISS is governed by the geometry of the CNT
- The cut-off distance of the L-J has a marginal effect on ISS
- Incorporation of an end cap in the pull-out test leads to a greater pull-out peaks